

Superconductivity without hole-pocket in electron-doped FeSe: Analysis beyond the Migdal-Eliashberg formalism

Youichi Yamakawa, and Hiroshi Kontani*

Department of Physics, Nagoya University, Furo-cho, Nagoya 464-8602, Japan.

(Dated: January 21, 2022)

High- T_c pairing mechanism absent of hole-pockets in heavily electron-doped FeSe is one of the key unsolved problems in Fe-based superconductors. Here, this problem is attacked by focusing on the higher-order many-body effects neglected in conventional Migdal-Eliashberg formalism. We uncover two significant many-body effects for high- T_c superconductivity: (i) Due to the “vertex correction”, the dressed multiorbital Coulomb interaction acquires prominent orbital dependence for low-energy electrons. The dressed Coulomb interaction not only induces the orbital fluctuations, but also magnifies the electron-boson coupling constant. Therefore, moderate orbital fluctuations give strong attractive pairing interaction. (ii) The “multi-fluctuation-exchange pairing process” causes large inter-pocket attractive force, which is as important as usual single-fluctuation-exchange process. Due to these two significant effects dropped in the Migdal-Eliashberg formalism, the anisotropic s_{++} -wave state in heavily electron-doped FeSe is satisfactorily explained. The proposed “inter-electron-pocket pairing mechanism” will enlarge T_c in other Fe-based superconductors.

PACS numbers: 74.70.Xa, 75.25.Dk, 74.20.Pq

I. INTRODUCTION

The pairing mechanism in Fe-based superconductors is a significant unsolved issue in condensed matter physics. Strong spin and/or orbital fluctuations are expected to mediate the pairing interaction [1–7]. To achieve a convincing answer on this problem, normal state electronic states should be clearly understood, and therefore the electronic nematic state has been studied very actively. The nematic state is the spontaneous rotational symmetry breaking driven by the electron correlation that triggers the small lattice distortion at $T = T_{\text{str}}$. Large orbital polarization ($E_{yz} - E_{xz} \sim 60\text{meV}$) is observed by the angle-resolved-photoemission spectroscopy (ARPES) [8, 9]. To explain the nematic phase in Fe-based superconductors, various theoretical possibilities have been proposed so far. Both the spin-nematic scenario [10, 11] and the orbital/charge order scenario [12–15] have been discussed very actively.

In the latter scenario, it is difficult to derive the orbital/charge order based on the conventional mean-field-level theories, like the random-phase-approximation (RPA). This fact means that the higher-order electronic correlations, called the vertex corrections (VCs), should play essential roles on the nematic transition [14]. The Fermi liquid theory tells that the dressed Coulomb interaction due to the VCs can acquire nontrivial spin- and orbital-dependences for low-energy electrons [16, 17]. In Fe-based superconductors, the orbital-dependent dressed Coulomb interaction has been discussed in Refs. [18–21].

In Ref. [14], the authors found the significant role of the Aslamazov-Larkin (AL) type VC for the bare Coulomb interaction \hat{U}^0 , which we call the U -VC in this paper. Since the AL-type U -VC enlarges the “inter-orbital repulsive interaction” under moderate spin fluctuations [14, 22, 23], the orbital order is driven by the electron correlation in Fe-based superconductors. In Refs.

[24, 25], this mechanism has been applied to explain the nematic charge-density-wave in cuprate superconductors, which has been a significant open problem in strongly-correlated electron systems [26, 27].

Considering the importance of the U -VC in the normal state [14, 15], the same U -VC should have strong impact on the superconductivity. In conventional spin/orbital-fluctuation pairing theories, the coupling constant between the electron and the fluctuations (= bosons) is simply given by the bare interaction \hat{U}^0 [1], which we call the “Migdal approximation” in this manuscript. However, the fluctuation-mediated pairing interaction is modified by the U -VCs for the electron-boson coupling constant, which is expected to be important in Fe-based superconductors. Therefore, we have to formulate the “gap equation beyond the Migdal-Eliashberg (ME) theory” by considering the U -VC seriously. This is the main topic of the present study.

Among the Fe-based superconductors, FeSe families attract considerable attention because of its high potential for realizing high- T_c superconducting state. To explain the nematic state without magnetization in FeSe, the spin-nematic [28–30] and the orbital-order [22, 23, 31–33] mechanisms have been discussed. [34, 35] whereas strong “nematic fluctuations” are observed by the shear modulus and B_{1g} electronic Raman study [35–37]. Below T_{str} , large orbital polarization appears with the unconventional sign-reversal in \mathbf{k} -space [23, 32, 33, 38]. These characteristic non-magnetic nematic states above and below T_{str} are quantitatively explained by considering the U -VC, using the self-consistent VC (SC-VC) theory [22, 23].

In FeSe, high- T_c state emerges by introducing 10 ~ 15% electron carrier, as observed in ultrathin FeSe on SrTiO_3 ($T_c = 40 \sim 100\text{K}$) [39–43], K-coated FeSe ($T_c \lesssim 50\text{K}$) [44, 45], and intercalated superconductor $(\text{Li}_{0.8}\text{Fe}_{0.2})\text{OHFeSe}$ ($T_c \lesssim 40\text{K}$) [46, 47]. The fully-

gapped s -wave state has been confirmed experimentally [42, 43, 47], and the sign-preserving s_{++} -wave state is reported in Refs. [42, 46]. In these high- T_c compounds, the top of the hole-pocket completely sinks below the Fermi level ($\sim -0.1\text{eV}$). Although strong interfacial electron-phonon interaction may increase T_c in FeSe film on SrTiO_3 [48–52], its importance is not clear for other electron-doped FeSe. Thus, it is a significant unsolved problem to explain the high- T_c s -wave state without hole-pockets based on the repulsive Coulomb interaction.

In this paper, we study the high- T_c pairing mechanism for heavily electron-doped (e -doped) FeSe. Even in the absence of the hole-pocket, we find that moderate spin and orbital fluctuations develop, due to the orbital-spin interplay through the U -VC. Then, moderate orbital fluctuations give rise to strong attractive pairing interaction since the electron-boson coupling constant is dressed and magnified by the U -VC. In addition, the AL-type multi-fluctuation-exchange pairing process causes large inter-pocket attractive force, which is not simply proportional to the single-fluctuation-exchange process. Because of these beyond-ME pairing mechanisms uncovered by the present study, the fully-gapped s_{++} -wave state is naturally obtained. The obtained anisotropic gap structure is consistent with experimental results [42, 43, 46, 47].

The s_{++} -wave state in heavily e -doped compounds due to the charge-channel fluctuations was discussed based on phenomenological approaches [53, 54]. Here, we analyze the realistic Hubbard model using the advanced microscopic theory, and uncover the beyond-ME pairing mechanism responsible for the strong attractive pairing interaction.

The nematic orbital order is driven by the combination of the VC due to the electron correlation and the electron-phonon interaction. In Fe-based superconductors, the electron correlation effect is the main driving force of the nematic transition, as theoretically explained in Ref. [15].

II. VERTEX CORRECTIONS IN MULTIORBITAL SYSTEMS BASED ON THE FERMI LIQUID THEORY

We first introduce the U -VC, which expresses the three-point vertex connecting between the electron and the fluctuations. We show that the U -VC strongly modifies the essential electronic properties in strongly correlated electron systems. In multiorbital systems, the Coulomb interaction is represented by the intra-orbital term U , the inter-orbital term U' , and the exchange or Hund's coupling term J . Its matrix expression, \hat{U}^{0x} , is given in Fig. 1 (a) [1, 14], where $x = c, s$ represents the charge- or spin-channel interaction. Its expression for Fe-based superconductors is given in the next section. (Note that $U^{0s} = -U^{0c} = U$ in the single-orbital case.)

Due to the many-body effect, the model interaction is changed to energy- and momentum-dependent dressed

interaction $\hat{U}^x(k, p)$, where $k = (\epsilon_n = (2n+1)\pi T, \mathbf{k})$ and $p = (\epsilon_m, \mathbf{p})$. The lowest few terms for the three-point vertex (U -VC) are shown in Fig. 1 (b). The solid lines are the electron Green functions. The dressed interaction is expressed as $\hat{\Lambda}^x(k, p)\hat{U}^{0x}$, and we call $\hat{\Lambda}^x(k, p)$ the x -channel U -VC. Note that the U -VC is irreducible with respect to \hat{U}^{0x} , and $\Lambda_{l,l';m,m'}^x = \delta_{l,m}\delta_{l',m'} \equiv \hat{1}$ in the Migdal approximation.

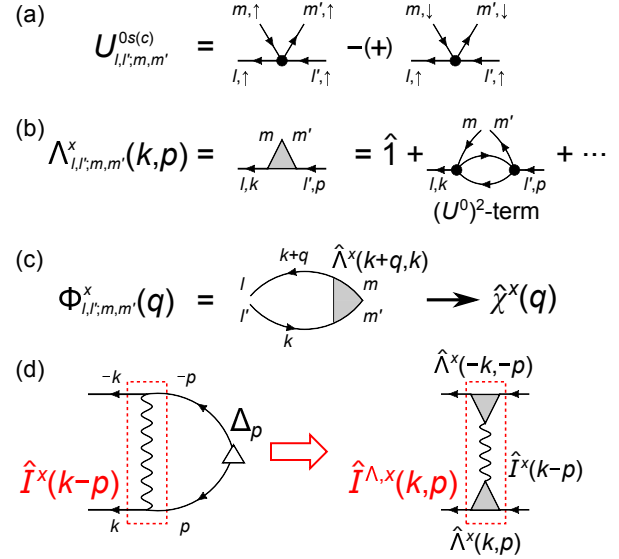


FIG. 1: (color online) (a) The Hubbard interaction for the spin- (charge-) channel $\hat{U}^{0s(c)}$, denoted as the black circle. (b) The three-point VC for the coupling constant between the electron and the fluctuations (U -VC), $\Lambda_{l,l';m,m'}^x(k, p)$ ($x = s, c$). ($\hat{\Lambda}^x = \hat{1}$ for $U \rightarrow 0$.) The (U^0) -linear terms are dropped since they are included in the RPA diagrams. The dressed coupling constant modified by the U -VC is $\hat{U}^x(k, p) = \hat{\Lambda}^x(k, p)\hat{U}^{0x}$. (c) Beyond the RPA: $\hat{\Phi}^x(q)$ is the irreducible susceptibility with the VC. (d) Single-fluctuation-exchange pairing interaction beyond the ME approximation. The U -VC is given by Eq. (4).

The significance of the U -VC in Fe-based superconductors was discovered in Ref. [14]: Strong orbital fluctuations arise from the U -VC that is included in the irreducible charge susceptibility

$$\hat{\Phi}_{l,l';m,m'}^x(q) = -T \sum_{k,l_1,l_2} G_{l,l_1}(k+q) G_{l_2,l'}(k) \times \Lambda_{l_1,l_2;m,m'}^x(k+q,k), \quad (1)$$

which is illustrated in Fig. 1 (c). Here, $q = (\omega_l = 2\pi lT, \mathbf{q})$. Then, the susceptibility

$$\hat{\chi}^x(q) = \hat{\Phi}^x(q)[\hat{1} - \hat{U}^{0x}\hat{\Phi}^x(q)]^{-1} \quad (x = s, c), \quad (2)$$

is strongly influenced by the U -VC included in $\hat{\Phi}^x(q)$. The magnetic (orbital) order occurs when the spin (charge) Stoner factor α_S (α_C), which is given as the maximum eigenvalue of $\hat{U}^{s(c)}\hat{\Phi}^{s(c)}(q)$, reaches unity.

The U -VC should also be significant for the superconductivity: Conventionally, the pairing interaction due to the single-fluctuation-exchange (=Maki-Thompson process) is studied, and the U -VC for the electron-boson coupling is dropped (=Migdal approximation). Then, the interaction due to charge or spin susceptibility χ^x is

$$\hat{I}^x(k-p) = \hat{U}^{0x} + \hat{U}^{0x} \hat{\chi}^x(k-p) \hat{U}^{0x}, \quad (3)$$

where $x = c$ (charge) or $x = s$ (spin). However, the bare electron-boson coupling should be dressed by the U -VC as shown in Fig. 1 (d), which is required by the microscopic Fermi liquid theory [55]. The pairing interaction with the U -VC (=beyond Migdal approximation) is given as

$$\hat{I}^{\Lambda,x}(k,p) = \hat{\Lambda}^x(k,p) \hat{I}^x(k-p) \hat{\Lambda}^x(-k,-p), \quad (4)$$

where $\bar{\Lambda}_{l,l';m,m'}^x(k,p) \equiv \Lambda_{m',m;l,l'}^x(k,p)$. Its expression is illustrated in Fig. 1 (d). We stress that $\hat{\Lambda}^x$ and $\hat{\Phi}^x$ are exactly related by the one-to-one relationship $\hat{\Phi}^x(q) = -T \sum_k \hat{G}(k+q) \hat{G}(k) \hat{\Lambda}^x(k+q, k)$.

III. MODEL HAMILTONIAN FOR 15% E-DOPED FESE

In this paper, we analyzed the eight-orbital Hubbard model for heavily e -doped FeSe model:

$$H = H_0 + rH_U. \quad (5)$$

Here, H_0 is the kinetic term, which we will introduce below, and H_U is the first-principles multiorbital interaction for FeSe [56]. The factor r is the reduction factor for the interaction term [22].

The kinetic term H_0 is given as

$$H_0 = \sum_{\mathbf{k}, l, l', \sigma} c_{\mathbf{k}, l, \sigma}^\dagger H_{\mathbf{k}, l, l'}^{0, b} c_{\mathbf{k}, l', \sigma} + \Delta H^0 \quad (6)$$

where $H_{\mathbf{k}, l, l'}^{0, b}$ is the tight-binding model for the bulk FeSe introduced in Ref. [22]. Here, l is the orbital index, and we denote $d_{z^2}, d_{xz}, d_{yz}, d_{xy}, d_{x^2-y^2}$ orbitals as 1, 2, 3, 4, 5, and p_x, p_y, p_z orbitals as 6, 7, 8. In bulk FeSe, the relation $E_{xy} < E_{yz} (< \mu)$ holds at X point. In e -doped FeSe, however, the opposite relation $E_{xy} > E_{yz}$ holds, and the Fermi velocity is much smaller [49, 57]. We introduce ΔH^0 in order to reproduce the experimental bandstructure and FSs in e -doped FeSe, we shift the E_{xz} [E_{xy}] level at $\mathbf{k} = ((0, 0), (\pi/2, 0), (\pi, 0), (0, \pi/2), (\pi/2, \pi/2), (\pi, \pi/2), (0, \pi), (\pi/2, \pi), (\pi, \pi))$ by $(+0.2, 0, 0, 0, 0, 0, +0.2, 0, 0)$ [$(+0.25, -0.1, +0.4, -0.1, 0, 0, +0.4, 0, 0)$] in unit eV, by introducing the additional intra-orbital hopping integrals for $l = 2 \sim 4$.

Figure 2 (a) shows the bandstructure and FSs, which are unfolded in the present 1-Fe unit cell (1Fe-UC) model. In this paper, we introduce the orbital-dependent renormalization factors $z_4 = 1/1.6$ and $z_l = 1$ ($l \neq 4$) [22]:

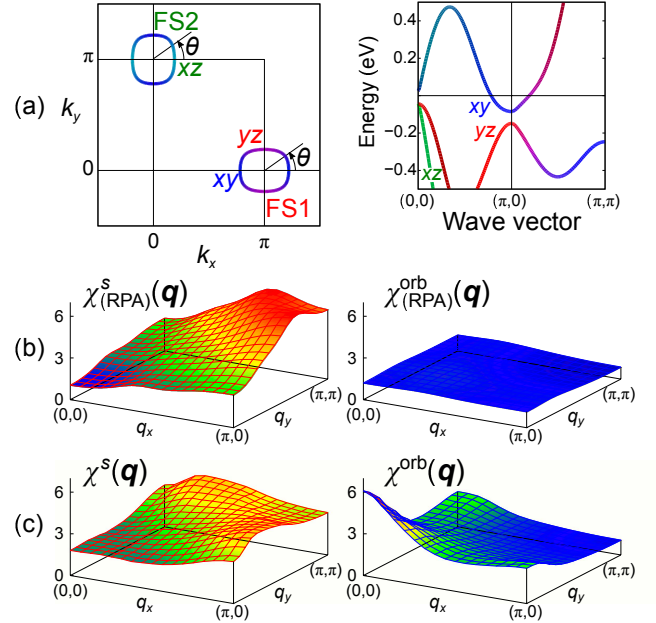


FIG. 2: (color online) (a) FSs and bandstructure of the 1Fe-UC FeSe model with 15% e -doping. Green, red, and blue lines correspond to xz , yz , and xy orbitals, respectively. In each FS, the xy -orbital has large weight near the k_x - or k_y -axis. (b) The spin and orbital susceptibilities obtained by the RPA. The latter is very small in the RPA. (c) The spin and orbital susceptibilities obtained by the SC-VC theory. The U -VCs for the irreducible susceptibilities $\hat{\Phi}^{s,c}(q)$ are calculated self-consistently. Moderate ferro-orbital fluctuations are induced by the charge-channel U -VC, consistently with the experimental phase diagram of e -doped FeSe.

Consistently, the relation $z_{2,3}/z_4 \sim 1.3$ is given by the dynamical-mean-field-theory in Ref. [58]. The band dispersion is given by the pole of the Green function $\hat{G}(\mathbf{k}, \epsilon) = (\hat{Z} \cdot \epsilon - \hat{H}_0(\mathbf{k}))^{-1}$, where $Z_{l,m} = (1/z_l) \delta_{l,m}$ [22, 23]. Equivalently, it is given by the eigenvalues of $\hat{Z}^{-1/2} \hat{H}_0(\mathbf{k}) \hat{Z}^{-1/2}$.

The Coulomb interaction term for d -electrons H_U is expressed as

$$H_U = -\frac{1}{2} \sum_{i, l, l', m, m'} \sum_{\sigma \rho} U_{l\sigma, l'\sigma; m\rho, m'\rho}^0 c_{i, l\sigma}^\dagger c_{i, l'\sigma} c_{i, m'\rho}^\dagger c_{i, m\rho}, \quad (7)$$

where

$$U_{l\sigma, l'\sigma'; m\rho, m'\rho'}^0 = \frac{1}{2} U_{l, l'; m, m'}^{0c} \delta_{\sigma, \sigma'} \delta_{\rho, \rho'} + \frac{1}{2} U_{l, l'; m, m'}^{0s} \boldsymbol{\sigma}_{\sigma, \sigma'} \cdot \boldsymbol{\sigma}_{\rho', \rho}, \quad (8)$$

where $\boldsymbol{\sigma} = (\sigma_x, \sigma_y, \sigma_z)$ is the Pauli matrix vector. The relationship with respect to the spin indices in Eq. (8) is rigorous even for the dressed four-point vertex function, by reflecting the $SU(2)$ symmetry in the absence of the SOI [55]. In addition, the relationship $\hat{U}_{l, l'; m, m'}^{0s} - \hat{U}_{l, l'; m, m'}^{0c} = 2\hat{U}_{l, m; l', m'}^{0s}$ holds.

\hat{U}^{0s} and \hat{U}^{0c} is the matrix expression for the multi-orbital interaction for the spin or charge channel introduced in Refs. [1, 14, 22]:

$$U_{l,l';m,m'}^{0s} = \begin{cases} U_{l,l}, & l = l' = m = m' \\ U'_{l,l'}, & l = m \neq l' = m' \\ J_{l,m}, & l = l' \neq m = m' \\ J_{l,l'}, & l = m' \neq l' = m \\ 0, & \text{otherwise,} \end{cases} \quad (9)$$

and

$$U_{l,l';m,m'}^{0c} = \begin{cases} -U_{l,l}, & l = l' = m = m' \\ U'_{l,l'} - 2J_{l,l'}, & l = m \neq l' = m' \\ -2U'_{l,m} + J_{l,m}, & l = l' \neq m = m' \\ -J_{l,l'}, & l = m' \neq l' = m \\ 0, & \text{otherwise.} \end{cases} \quad (10)$$

Here, $U_{l,l}$, $U'_{l,l'}$ and $J_{l,l'}$ are the first-principles Coulomb interaction terms for FeSe obtained in Ref. [56].

IV. ORBITAL AND SPIN SUSCEPTIBILITIES

From now on, we perform the numerical study for the spin- and orbital susceptibilities in the 15% e-doped FeSe model shown in Fig. 2 (a). They are given by Eqs. (1) and (2). In the RPA, the U -VC is dropped ($\hat{\Lambda}^x = \hat{1}$), so $\hat{\Phi}^x(q)$ is reduced to the bare susceptibility $\chi_{l,l';m,m'}^0(q) = -T \sum_k G_{l,m}(k+q) G_{m',l'}(k)$. In this case, the relation $\alpha_S > \alpha_C$ holds, and therefore the non-magnetic orbital order failed to be explained.

In Fig. 2 (b), we show the the RPA results for the total spin susceptibility, $\chi^s(\mathbf{q}) \equiv \sum_{l,m}^{1 \sim 5} \chi_{l,l';m,m}^s(\mathbf{q})$, and the orbital susceptibility for the operator $\hat{O} \equiv n_{xz} - n_{yz}$, $\chi^{\text{orb}}(\mathbf{q}) \equiv \sum_{l,m}^{2,3} (-1)^{l+m} \chi_{l,l';m,m}^c(\mathbf{q})$. The model parameters are $r = 0.26$ and $T = 30$ meV. The spin and charge Stoner factors are $(\alpha_S, \alpha_C) = (0.80, 0.48)$. The broad incommensurate peak in $\chi_{(\text{RPA})}^s(\mathbf{q})$ originates from the multiple nesting vectors, such as the inter- and intra-pocket nestings in addition to the contribution from the hole-pockets sink below the Fermi level. $\chi_{(\text{RPA})}^{\text{orb}}(\mathbf{q})$ remains small in the RPA.

By going beyond the RPA, the opposite relation $\alpha_C > \alpha_S$ can be realized when the U -VC for the charge channel becomes greater than $\hat{1}$. In the SC-VC theory, the diagrammatic expression for $\hat{\Lambda}^x$ is shown in Fig. 3, in which all the diagrams up to $O((\chi^x)^2)$ are calculated self-consistently. The analytic expressions for U -VC are explained in Appendix A. Based on the SC-VC theory, we can explain the strong development of the orbital fluctuations in Fe-based superconductors since $\hat{\Phi}^c(q)$ for the $d_{xz/yz}$ -orbitals is enlarged by the charge-channel U -VC [14, 22].

The RPA results are qualitatively modified by the U -VC: In Fig. 2 (c), we show $\chi^s(\mathbf{q})$ and $\chi^{\text{orb}}(\mathbf{q})$ obtained

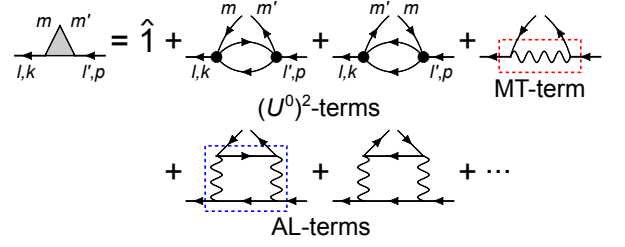


FIG. 3: (color online) Diagrammatic expression for the U -VC analyzed in the present theoretical study. Double counting terms are subtracted carefully. The MT (AL) diagram inside the red (blue) dotted rectangle corresponds to the MT (AL) diagram in the pairing interaction in Fig. 1 (d) (Fig. 5 (e)).

by the SC-VC theory for $r = 0.35$ at $T = 30$ meV, where the obtained Stoner factors are $(\alpha_S, \alpha_C) = (0.83, 0.81)$. Due to AL type U -VC in Φ^c , $\chi^c(\mathbf{q})$ shows moderate peak at $\mathbf{q} \sim (0, 0)$, consistently with the experimental phase diagram of e-doped FeSe [45]. Also, the \mathbf{q} -dependence of $\chi^s(\mathbf{q})$ is weakly modified from the RPA result due to the U -VC in Φ^s . More detailed numerical results obtained by the SC-VC theory are explained in Appendix B.

V. GAP EQUATION AND PAIRING INTERACTION BEYOND THE ME FORMALISM

Here, we study the following linearized gap equation in the band-diagonal basis:

$$\lambda \Delta_\alpha(k) = -T \sum_{p,\beta} V_{\alpha,\beta}^{\text{SC}}(k,p) |G_\beta(p)|^2 \Delta_\beta(p), \quad (11)$$

where $\Delta_\alpha(k)$ is the gap function on the α -band, λ is the eigenvalue, which is proportional to T_c , and $\lambda = 1$ is satisfied at $T = T_c$. $V_{\alpha,\beta}^{\text{SC}}$ is the pairing interaction in the band-diagonal basis. For the singlet case, the pairing interaction with the U -VC is given by

$$\hat{V}^\Lambda(k,p) = \frac{3}{2} \hat{I}^{\Lambda,s}(k,p) - \frac{1}{2} \hat{I}^{\Lambda,c}(k,p) - \hat{U}^{0s}, \quad (12)$$

where $I^{\Lambda,x}$ is given in Eq. (4) using the SC-VC susceptibilities. The (U^0) -linear term of Eq. (12) is $\frac{1}{2} [\hat{U}^{0s} - \hat{U}^{0c}]$.

Before analyzing Eq. (11) numerically, we briefly discuss the possible gap states in heavily e-doped FeSe [48, 54]: Since the hole-FSs are absent, the only possible states are the s -wave and d -wave states, shown in Fig. 4 (a). The former (latter) state is realized when the inter-pocket pairing interaction is attractive (repulsive), which may be mediated by the orbital (spin) fluctuations. Next, we study the realistic 2Fe-UC model to understand the effect of the spin-orbit interaction (SOI) $\lambda_{\text{SOI}} \mathbf{l} \cdot \mathbf{s}$. Due to the SOI-induced hybridization between FS1 and FS2, the d -wave state possesses the nodal gap structure as schematically shown in Fig. 4 (b), accompanied by drastic decrease in T_c [48]. On the other hand, the s -wave state is essentially insensitive to the SOI-hybridization.

In addition, the s_{\pm} -wave state in Fig. 4 (c) was discussed theoretically [59].

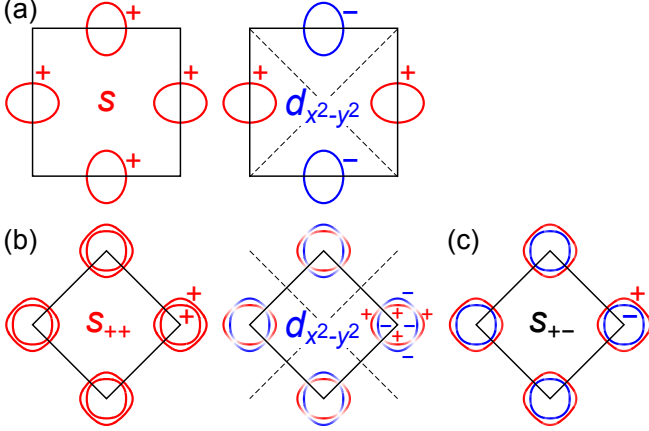


FIG. 4: (color online) (a) The schematic fully-gapped s -wave and d -wave states in the 1Fe-UC Brillouin zone. For former (latter) is realized when the inter-pocket pairing interaction is attractive (repulsive). (b) The s_{++} -wave state and d -wave state in the 2Fe-UC Brillouin zone. The inner FS and outer FS are formed due to the SOI-induced band hybridization. In the d -wave state, the gap structure becomes nodal and T_c is suppressed due to the SOI-induced hybridization [48]. (c) The s_{\pm} -wave state discussed in Ref. [59].

Here, we explain the significance of the U -VCs for the pairing interaction in Eq. (4). In Fig. 5, we show the obtained (a) $|\Lambda_{3,3,3,3}^c|^2$ and (b) $|\Lambda_{4,4,4,4}^s|^2$ on the FSs in 15% e -doped FeSe model, in the case of $r = 0.35$ [$(\alpha_S, \alpha_C) = (0.80, 0.73)$] at $T = 30$ meV. Their analytic expressions are given in Appendix A. In these figures, θ and θ' represent the momenta on the FSs \mathbf{k} and \mathbf{p} respectively. It is found that $|\Lambda_{3,3,3,3}^c(\mathbf{k}, \mathbf{p})|^2 \lesssim 4$ for the intra-pocket ($\mathbf{k}, \mathbf{p} \in \text{FS1}$). Then, $V^{\Lambda, c}$ gives strong attractive interaction under moderate spin fluctuations. Such large charge-channel U -VC originates from the AL-type VC, consistently with the functional-renormalization-group analysis in Ref. [55] based on the functional-renormalization-group method. In contrast, the opposite relation holds for the spin-channel U -VC; $|\Lambda_{4,4,4,4}^s(\mathbf{k}, \mathbf{p})|^2 \lesssim 0.35$ for the inter-pocket ($\mathbf{k} \in \text{FS1}, \mathbf{p} \in \text{FS2}$). Thus, spin-fluctuation-mediated inter-pocket repulsion is reduced by the spin-channel U -VC [55].

Next, we study the pairing interaction. In the RPA without any U -VC, $V_{\text{RPA}}(\mathbf{k}, \mathbf{p})$, both intra- and inter-pocket interactions are positive (=repulsive), as shown in Fig. 5 (c). However, as shown in Fig. 5 (d), the intra-pocket interaction becomes negative (=attractive) for $V^{\Lambda}(\mathbf{k}, \mathbf{p})$ in the presence of U -VCs, since the pairing force due to the orbital fluctuations is multiplied by $|\Lambda^c|^2 \gg 1$. Since the averaged inter-pocket interaction is tiny, s -wave state and d -wave state are approximately degenerate. (see Fig. 7 (b) without SOI.) In Figs. 5 (c) and (d), the frequency-independent (\hat{U}^0)-linear term is dropped, although it is included in solving the gap equation below.

Up to now, we analyzed only the single-fluctuation-exchange processes. We also find that large attractive interaction is given by the “AL-type crossing-fluctuation-exchange process” $\hat{V}^{\text{cross}}(k, p)$ shown in Fig. 5 (e). Its significance is naturally expected since \hat{V}^{cross} is mathematically equivalent to the AL-VC that plays significant role in the present multiorbital system [14]. Physically, $V^{\text{cross}}(k, p)$ represents the pairing glue due to the “multi-boson-exchange processes”. In the orbital basis, its analytic expression is

$$V_{l,l',m,m'}^{\text{cross}}(k, p) = \frac{T}{4} \sum_q \sum_{a,b,c,d} G_{a,b}(p-q) G_{c,d}(-k-q) \times \{ 3I_{l,a;m,d}^{\prime s}(k-p+q) I_{b,l';c,m'}^{\prime s}(-q) + 3I_{l,a;m,d}^{\prime s}(k-p+q) I_{b,l';c,m'}^{\prime c}(-q) + 3I_{l,a;m,d}^{\prime c}(k-p+q) I_{b,l';c,m'}^{\prime s}(-q) - I_{l,a;m,d}^{\prime c}(k-p+q) I_{b,l';c,m'}^{\prime c}(-q) \}, \quad (13)$$

where we put $\hat{I}'^x = \hat{I}^x - \hat{U}^0 x$ to avoid the double counting of diagrams included in other terms. This analytic expression is essentially the same as that for the AL-type U -VC in Fig. 3. so $V^{\text{cross}}(k, p)$ is naturally expected to be important in Fe-based superconductors.

To understand why $\hat{V}^{\text{cross}}(k, p)$ becomes negative, we consider the case that $V^{s,c}$ has moderate energy dependence. By dropping the orbital indices of $V^{s,c}$ for simplicity, we obtain

$$V^{\text{cross}}(\mathbf{k}, \mathbf{p}) \approx - \sum_q \frac{f_{\mathbf{k}-\mathbf{q}} - f_{\mathbf{p}-\mathbf{q}}}{\epsilon_{\mathbf{p}-\mathbf{q}} - \epsilon_{\mathbf{k}-\mathbf{q}}} \{ 3I^s(\mathbf{q}) I^s(\mathbf{k} + \mathbf{p} - \mathbf{q}) + 3I^s(\mathbf{q}) I^c(\mathbf{k} + \mathbf{p} - \mathbf{q}) + 3I^c(\mathbf{q}) I^s(\mathbf{k} + \mathbf{p} - \mathbf{q}) - I^c(\mathbf{q}) I^c(\mathbf{k} + \mathbf{p} - \mathbf{q}) \}, \quad (14)$$

where $f_{\mathbf{k}}$ is the Fermi distribution function for $\epsilon = \epsilon_{\mathbf{k}}$. Then, $\frac{f_{\mathbf{k}-\mathbf{q}} - f_{\mathbf{p}-\mathbf{q}}}{\epsilon_{\mathbf{p}-\mathbf{q}} - \epsilon_{\mathbf{k}-\mathbf{q}}}$ is always positive. In a single-orbital model, $I^s(\mathbf{q}) \approx U/(1 - U\chi^{(0)}) > 0$ and $I^c(\mathbf{q}) \approx -U/(1 + U\chi^{(0)}) < 0$, so V^{cross} is small due to the cancellation, which can be verified numerically in the single-orbital Hubbard model for cuprate superconductors. In contrast, in the FeSe model, $I^c(\mathbf{q})_{m,m;m,m}$ has positive value even in the RPA. When $\chi^{\text{orb}} \gg 1$ due to the AL-VC, $I_{2,2;2,2}^c(\mathbf{q}) \sim -U + U^2 \chi^{\text{orb}}(\mathbf{q})/4$ takes large positive value for $J/U \ll 1$. Thus, V^{cross} gives the large negative interaction in the multiorbital model.

According to Eq. (14), $V_{m,m;m,m}^{\text{cross}}$ can take large negative value when the spin fluctuations develop on the m -orbital. In the present FeSe model, the magnitudes of $\chi_{m,m;m,m}^s$ for $m = 2 \sim 4$ are comparable. Since the d_{xy} -orbital is involved in both electron-pockets, $V_{4,4;4,4}^{\text{cross}}$ gives large attractive inter-pocket interaction in the present study.

Since Eq. (14) gives an over-estimated value, we perform the serious numerical analysis based on Eq. (14): Figure 5 (f) shows the obtained $\hat{V}^{\text{cross}}(\mathbf{k}, \mathbf{p})$ on the FSs. Since the total pairing interaction

$$\hat{V}^{\text{tot}}(k, p) = \hat{V}^{\Lambda}(k, p) + \hat{V}^{\text{cross}}(k, p), \quad (15)$$

is negative for both inter- and intra-pocket part, the s -wave state should appear. The significant role of V^{cross} is one of the main findings in the present study. It is verified that the momentum-dependence of $\hat{V}^{\text{cross}}(\mathbf{k}, \mathbf{p})$ given by Eq. (14) is similar to that given by Eq. (13). However, the former is over-estimated by two- or three-times.

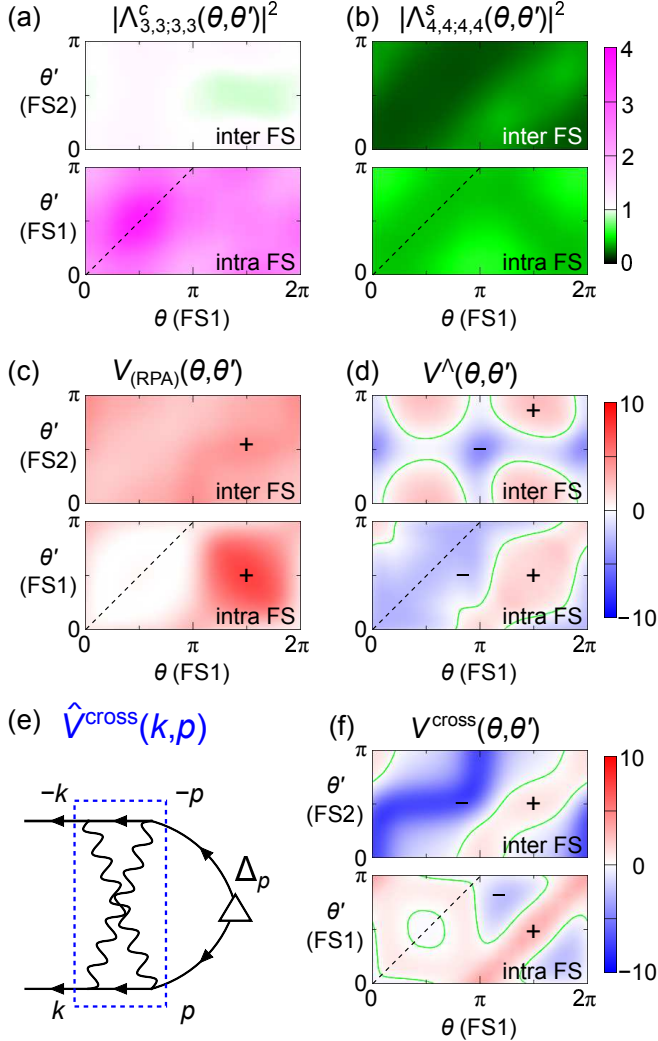


FIG. 5: (color online) (a) $|\Lambda_{3,3;3,3}^c(\theta, \theta')|^2 (\gg 1)$ and (b) $|\Lambda_{4,4;4,4}^s(\theta, \theta')|^2 (\ll 1)$ in e -doped FeSe model at the lowest frequency ($\epsilon_n = \epsilon_n' = \pi T$), where θ and θ' represent the Fermi momenta; see Fig. 2 (a). We show the pairing interactions (c) $V_{(\text{RPA})}$ and (d) V^Λ on the FSs. The summation for the lowest Matsubara frequencies ($\epsilon_n = \pm \epsilon_n' = \pi T$) is taken. The attractive interaction in (d) originates from the orbital fluctuations. (e) The crossing-fluctuation-exchange (=AL process) pairing interaction $V^{\text{cross}}(k, p)$, which represents the multi-fluctuation-exchange processes. (f) V^{cross} on the FSs, in which strong attractive inter-pocket interaction gives the s -wave state.

VI. S_{++} -WAVE GAP FUNCTION IN 15% E-DOPED FESE

From now on, we analyze the gap equation (11) numerically. We solve the frequency dependence of the gap function seriously, by restricting the momentum \mathbf{k}, \mathbf{p} on the FSs as done in Ref. [60]. In the absence of the SOI, the pairing interaction in the band-diagonal basis is

$$V_{\alpha,\beta}^{\text{tot}}(k, p) = \sum_{ll'mm'} V_{l,l';m,m'}^{\text{tot}}(k, p) \times u_{l\alpha}^*(\mathbf{k}) u_{l'\beta}(\mathbf{p}) u_{m\beta}(-\mathbf{p}) u_{m'\alpha}^*(-\mathbf{k}), \quad (16)$$

where $u_{l\alpha}(\mathbf{k}) = \langle \mathbf{k}; l | \mathbf{k}; \alpha \rangle$ is the unitary matrix connecting between the band representation and the orbital one. Then, the gap equation is rewritten as

$$\lambda z_\alpha^{-1}(\mathbf{k}) \Delta_\alpha(\mathbf{k}, \epsilon_n) = -\frac{\pi T}{(2\pi)^2} \sum_{\beta, m} \int_{\text{FS}\beta} \frac{d\mathbf{p}}{|v_\beta^\beta|} V_{\alpha,\beta}^{\text{tot}}(\mathbf{k}, \epsilon_n, \mathbf{p}, \epsilon_m) \times \frac{\Delta_\beta(\mathbf{p}, \epsilon_m)}{|\epsilon_m|}, \quad (17)$$

where λ is the eigenvalue. $z_\alpha(\mathbf{k}) = \sum_l z_l |u_{l\alpha}(\mathbf{k})|^2$ is the renormalization factor for band α . The gap equation in the presence of the SOI is explained in Sect. II C of Ref. [60]. In the numerical study, we calculate U -VCs in V^{tot} only for $|\epsilon_n| = |\epsilon_m| = \pi T$, and put $\hat{\Lambda}^{s,c} = \hat{1}$ for others. This simplification is unfavorable for obtaining the s_{++} -wave state. Nonetheless of this underestimation, the s_{++} -wave state is realized in Fig. 6 (f) in the main text.

First, we study the 1Fe-UC model without the SOI shown in Fig. 2 (a): In the RPA without any U -VC, $V^{\text{SC}} = V_{(\text{RPA})}$, the spin-fluctuation-mediated d -wave state is obtained in Fig. 6 (a). Here, $|\Delta(\theta)|$ takes maximum on the region with large d_{xy} -orbital weight due to large spin fluctuations on the d_{xy} -orbital. However, the eigenvalue for the d -wave is just $\lambda^d = 0.26$ since the spin fluctuations are weak.

On the other hand, the s -wave state is obtained if the U -VC is taken into account, $V^{\text{SC}} = V^\Lambda$, shown in Fig. 6 (b). Here, the pairing interaction in Eq. (12), which is shown in Fig. 5 (d), is given by $\Lambda^{s,c}$ and $\hat{\chi}^{s,c}(q)$ obtained by the SC-VC theory. However, eigenvalue is still small ($\lambda^s = 0.37$) due to the cancellation in the inter-pocket interaction; see Figs. 5 (d). As we show in Fig. 6 (c), the s -wave state with large eigenvalue ($\lambda^s = 0.70$) is obtained for the total pairing interaction $V^{\text{tot}} = V^\Lambda + V^{\text{cross}}$ in Eq. (15), because of the attractive force by the crossing term V^{cross} . Here, $|\Delta(\theta)|$ takes maximum on the d_{xy} -orbital character region because of the repulsive intra-pocket interaction on the $d_{xz(yz)}$ -orbital due to $\chi_{xz(yz)}^s(\mathbf{q})$ with small- q , in addition to the attractive inter-pocket interaction due to $V^{\text{cross}}(k, p)$ on the d_{xy} -orbital.

In the next stage, we analyze the gap equation in the 2Fe-UC FeSe model with the SOI, by following the theoretical procedure in Ref. [60]. Figure 6 (d) shows the

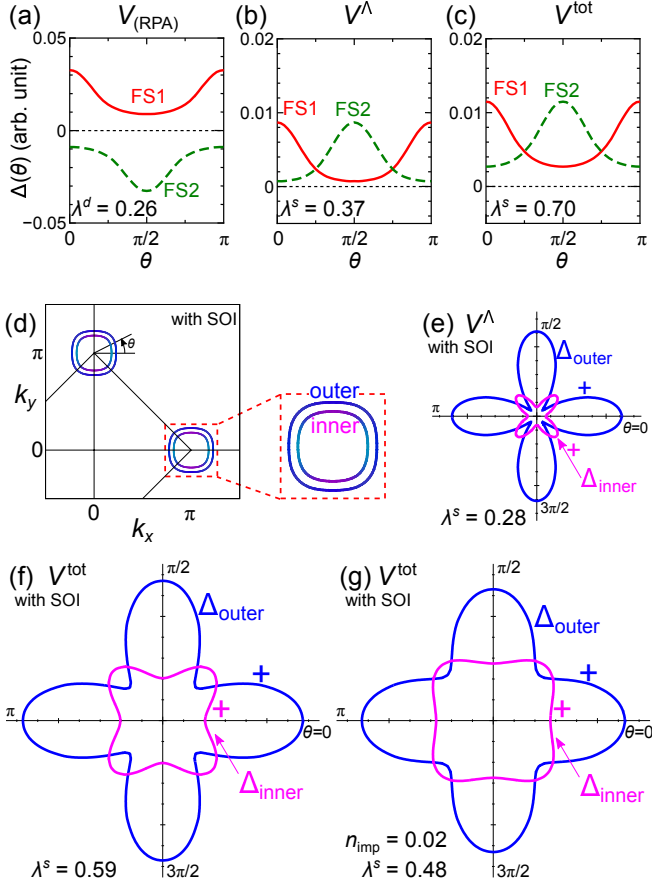


FIG. 6: (color online) The gap functions in the 1Fe-UC FeSe model obtained for the pairing interaction (a) V_{RPA} (b) V^Λ (with U -VC) and (c) V^{tot} (with U -VC and crossing term), without the SOI. In (b) and (c), the s -wave state is realized due to the orbital fluctuations. In all cases, the gap function has maximum on the region with strong d_{xy} -orbital character. (d) FSs in the 2Fe-UC FeSe model for $\lambda_{\text{SOI}} = 80$ meV. The outer (inner) FS is mainly composed of the xy -orbital (xz, yz -orbitals). We present the obtained s_{++} -wave gap functions for (e) V^Λ and (f) V^{tot} . (g) The s_{++} -wave state in the presence of impurities, by which the gap anisotropy is smeared. The anisotropic s_{++} -wave states in (f) and (g) are consistent with the experimental reports [42, 43, 46, 47].

FSs for $\lambda_{\text{SOI}} = 80$ meV. Due to the SOI-induced hybridization, very anisotropic s_{++} -wave state is obtained for $V^{\text{SC}} = V^\Lambda$, as shown in Fig. 6 (e). Figure 6 (f) shows the moderately anisotropic s_{++} -wave state obtained for $V^{\text{SC}} = V^{\text{tot}}$ [$\lambda^s = 0.59$]. The anisotropy of the s_{++} -wave state is smeared out by introducing small amount of the impurity as well-known: Figure 6 (g) show the s_{++} -wave state in the presence of the 2% impurity with the constant inter- and intra-pocket scattering potential $I_{\text{inter}} = I_{\text{intra}} = 1$ eV in the Born approximation. Thus, s_{++} -wave state with large λ^s is obtained under moderate spin and orbital fluctuations. The anisotropic s -wave states in Figs. 6 (f) and (g) are consistent with the experimental reports in Refs. [42, 43, 46, 47].

VII. ROBUSTNESS OF THE s -WAVE STATE

In the previous section, we performed the numerical study of the gap equation for the 15% e -doped FeSe model. The obtained anisotropic s_{++} -wave state shown in Fig. 6 is quantitatively consistent with experiments. In Fig. 6, we showed the numerical results only for $r = 0.35$ at $T = 30$ meV.

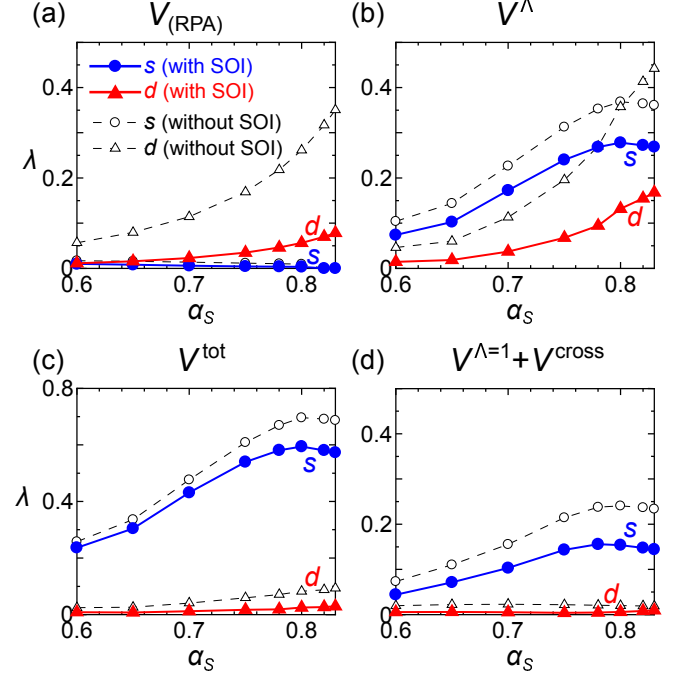


FIG. 7: (color online) The eigenvalue for the s -wave state λ^s and that for the d -wave state λ^d obtained for the pairing interaction (a) V_{RPA} , (b) V^Λ , and (c) V^{tot} . We also show the eigenvalues for (d) $V^{\text{SC}} = V^\Lambda + V^{\text{cross}}$.

Here, we explain that the s_{++} -wave state is obtained for wide parameter range. Figure 7 shows eigenvalues for the pairing interaction (a) V_{RPA} , (b) V^Λ , (c) V^{tot} , and (d) $V^\Lambda + V^{\text{cross}}$ as functions of α_S . In the RPA without any U -VC in Fig. 7 (a), the d -wave state is realized stably, whereas the eigenvalue for the d -wave state, λ^d , is strongly suppressed by the SOI. In Fig. 7 (b), we taking the U -VC into account. Due to the U -VC, λ^s increases drastically whereas λ^d is qualitatively unchanged compared to Fig. 7 (a). The reason is that the attractive intra-pocket force is enlarged by $|\Lambda^c|^2 \gg 1$, whereas the repulsive inter-pocket force is suppressed by $|\Lambda^s|^2 \ll 1$. In the presence of the SOI, the d -wave state is drastically suppressed, so the relation $\lambda^s > \lambda^d$ is realized.

The crossing term V^{cross} in Fig. 5 (e) or Eq. (13) gives large inter-pocket attractive interaction. Figure 7 (c) shows the eigenvalues for the pairing interaction $V^{\text{tot}} = V^\Lambda + V^{\text{cross}}$. Thanks to the strong attractive interaction by V^{cross} , λ^s is largely enlarged even in the absence of the SOI. Thus, the s_{++} -wave state is realized for wide range of α_S by going beyond the ME approxi-

mation.

We also show the s -wave and d -wave eigenvalues for $V^{\text{SC}} = V^{\Lambda=1} + V^{\text{cross}}$ in Fig. 7 (d). ($V^{\Lambda=1}$ represents the Migdal approximation. For V^{cross} , we replace each \hat{I}' in Eq. (13) with \hat{I} , and subtract the $(\hat{U}^0)^2$ -term.) In this case, the s -wave state is realized because of the attractive interaction by V^{cross} . However, the obtained λ^s is just ~ 0.3 . Thus, both U -VC and V^{cross} are necessary for explaining the fully-gapped s -wave state with large λ^s .

In summary, the s_{++} -wave state is obtained for wide parameter range in Fig. 7 (c) due to the combination of the U -VC and crossing term, even if the SOI is neglected. Once the SOI is taken into account correctly, the s_{++} -wave state is realized even if we drop either U -VC or V^{cross} but not both.

VIII. DISCUSSIONS

The mechanism of high- T_c superconductivity in Fe-based superconductors still remains an open problem. To attack this important issue, the high- T_c state ($T_c \gtrsim 60\text{K}$) without hole-pockets in heavily e -doped FeSe provides an excellent opportunity, since its very simple bandstructure is favorable for the unambiguous theoretical study. The only possible pairing states are s -wave state and d -wave state, and high- T_c state is realized irrespective of the small spin fluctuations [61]. Similar high- T_c with small spin fluctuations is realized in F- and H-doped LaFeAsO [62].

We analyzed the realistic Hubbard model for FeSe using the SC-VC theory, and found that moderately developed spin and orbital fluctuations appear for 15% e -doped case, consistently with the experimental phase diagram [45]. Next, we uncovered two significant “beyond-ME processes” for high- T_c pairing mechanism: (i) VC for the electron-boson coupling (U -VC), and (ii) AL-type crossing-fluctuation-exchange term (V^{cross}). Due to (i), strong intra-pocket attractive interaction is caused even when the ferro-orbital fluctuations are moderate. For this reason, T_c is enlarged for both d -wave and s -wave states. We stress that the phonon-mediated attractive interaction is also enlarged by the U -VC [55], so it is important to study the increment of T_c due to the electron-phonon mechanism [48, 49, 51]. Due to (ii), large inter-electron-pocket attractive interaction is realized. $V^{\text{cross}}(k, p)$ represents the pairing interaction due to the “multi-fluctuation-exchange processes”. Due to these beyond-ME processes, the fully-gapped s_{++} -wave state is satisfactorily explained. The obtained anisotropic gap structure is consistent with experimental results.

The significance of the U -VC in V^{Λ} has been verified in various multi-orbital Hubbard models [55, 63, 64]. In Ref. [55], we verified the significance of the U -VC by applying the functional-renormalization-group (fRG) method to the two-orbital Hubbard model: We showed that both the “ \mathbf{k} -dependence” and the “spin/charge-channel dependence” of the pairing interaction given by

the fRG four-point vertex are well approximated by the “single-fluctuation-exchange approximation with the U -VCs”. Although V^{cross} gives large attractive interaction in electron-doped FeSe model, its importance seems to be model-dependent. In fact, V^{cross} is less important in the two-orbital model [55] and in the undoped FeSe model studied in Ref. [64]. It is our important future problem to clarify the importance of the multi-fluctuation-exchange interactions in FeSe and other models, by using the fRG theory.

In Appendix C, we analyze the bulk FeSe model $\hat{H}_{\mathbf{k}}^{0,b}$ ($\Delta H^0 = 0$) with 15% e -doping, and obtain the full-gap s_{++} -wave state similar to Fig. 6 (f). However, the eigenvalue is only $\lambda^s = 0.22$. This result indicates that the change in the bandstructure in monolayer FeSe observed by ARPES, which is realized by lifting the d_{xy} -orbital level at X,Y points shown in Fig. 2 (a), is important to realize high- T_c superconductivity.

The present gap equation beyond the standard ME formalism should be useful for understanding the rich variety of the superconducting states in Fe-based superconductors. The proposed “inter-electron-pocket pairing mechanism” will enlarge T_c in other Fe-based superconductors, even if the s_{\pm} -wave state is realized.

Acknowledgments

We are grateful to A. Chubukov, P.J. Hirschfeld, R. Fernandes, J. Schmalian, Y. Matsuda, S. Shibauchi, and S. Onari for useful discussions. This study has been supported by Grants-in-Aid for Scientific Research from MEXT of Japan.

Appendix A: Analytic expressions for the U -VC in the SC-VC Theory

Here, we present the analytic expressions for the charge- and spin-channel U -VCs in the SC-VC theory. In the SC-VC theory, the U -VC for x -channel ($x = s, c$) is given as

$$\hat{\Lambda}^x(k, k') = \hat{1} + \hat{\Lambda}^{\text{MT},x}(k, k') + \hat{\Lambda}^{\text{AL},x}(k, k'), \quad (\text{A1})$$

where the index MT (AL) represents the MT (AL) term, shown in Fig. 3 in the main text.

First, we explain the MT-type U -VCs, which was already introduced in Ref. [55]. The charge- and spin-channel MT-terms are given as

$$\begin{aligned} \Lambda_{l,l';m,m'}^{\text{MT},c}(k, k') &= \frac{T}{2} \sum_p \sum_{a,b} \{ I_{b,l';a,l}^c(p) + 3I_{b,l';a,l}^s(p) \} \\ &\quad \times G_{a,m}(k+p) G_{m',b}(k'+p), \end{aligned} \quad (\text{A2})$$

$$\Lambda_{l,l';m,m'}^{\text{MT},s}(k, k') = \frac{T}{2} \sum_p \sum_{a,b} \{ I_{b,l';a,l}^c(p) - I_{b,l';a,l}^s(p) \}$$

$$\times G_{a,m}(k+p)G_{m',b}(k'+p), \quad (\text{A3})$$

where $\hat{I}^x(q) = \hat{U}^{0x}\hat{\chi}^x(q)\hat{U}^{0x} + \hat{U}^{0x}$, and a, b, l, l', m, m' are orbital indices.

Next, we explain the AL-type U -VCs, which was also introduced in Ref. [55]: The charge- and spin-channel AL-terms are given as

$$\begin{aligned} \Lambda_{l,l';m,m'}^{\text{AL},c}(k, k') &= \frac{T}{2} \sum_p \sum_{a,b,c,d,e,f} G_{a,b}(k'-p) \Lambda_{m,m';c,d,e,f}^{0'}(k-k', p) \\ &\times \{I_{l,a;c,d}^c(k-k'+p)I_{b,l';e,f}^c(-p) \\ &+ 3I_{l,a;c,d}^s(k-k'+p)I_{b,l';e,f}^s(-p)\}, \end{aligned} \quad (\text{A4})$$

$$\begin{aligned} \Lambda_{l,l';m,m'}^{\text{AL},s}(k, k') &= \frac{T}{2} \sum_p \sum_{a,b,c,d,e,f} G_{a,b}(k'-p) \Lambda_{m,m';c,d,e,f}^{0'}(k-k', p) \\ &\times \{I_{l,a;c,d}^c(k-k'+p)I_{b,l';e,f}^s(-p) \\ &+ I_{l,a;c,d}^s(k-k'+p)I_{b,l';e,f}^c(-p)\} \\ &+ \delta\Lambda_{l,l';m,m'}^{\text{AL},s}(k, k'), \end{aligned} \quad (\text{A5})$$

where the three-point vertex $\hat{\Lambda}^0(q, p)$ is given as

$$\begin{aligned} \Lambda_{l,l';a,b;e,f}^0(q, p) &= -T \sum_{k'} G_{l,a}(k'+q)G_{f,l'}(k')G_{b,e}(k'-p), \end{aligned} \quad (\text{A6})$$

and $\Lambda_{m,m';c,d;g,h}^{0'}(q, p) \equiv \Lambda_{c,h;m,g;d,m'}^0(q, p) + \Lambda_{g,d;m,c;h,m'}^0(q, -p-q)$. The last term in Eq. (A5) is given as

$$\begin{aligned} \delta\Lambda_{l,l';m,m'}^{\text{AL},s}(k, k') &= T \sum_p \sum_{a,b,c,d,e,f} G_{a,b}(k'-p) \\ &\times I_{l,a;c,d}^s(k-k'+p)I_{b,l';e,f}^s(-p)\Lambda_{m,m';c,d,e,f}^{0''}(k-k', p), \end{aligned} \quad (\text{A7})$$

where $\Lambda_{m,m';c,d;g,h}^{0''}(q, p) \equiv \Lambda_{c,h;m,g;d,m'}^0(q, p) - \Lambda_{g,d;m,c;h,m'}^0(q, -p-q)$. We verified that the contribution from Eq. (A7) is very small.

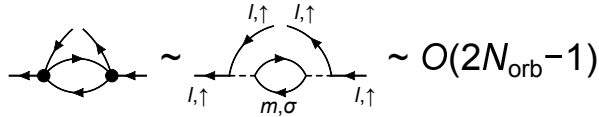


FIG. 8: (color online) The $(U^0)^2$ -term for the U -VC, by which the spin-channel U -VC is suppressed. One bubble scales as $\sim O(2N_{\text{orb}}-1)$, where N_{orb} is the d -orbital degrees of freedom.

Figure 3 represents the simplified diagrammatic expression for the U -VC, which is irreducible with respect to $\hat{U}^{0s(c)}$. The (U^0) -linear terms in Eqs. (A2) and (A3)

should be dropped to avoid the double counting of the RPA-type diagrams. We also carefully drop the double counting $(U^0)^2$ -terms included in both MT and AL terms.

We verified numerically that the large charge-channel U -VC ($|\Lambda^c|^2 \gg 1$) originates from the χ^s -square term in Eq. (A4). We also verified that the relation $|\Lambda^s|^2 \ll 1$ reported in the main text is mainly given by the $(U^0)^2$ -term in Fig. 8, since one bubble scales as $\sim O(2N_{\text{orb}}-1)$. This result is consistent with the previous analysis for the two-orbital model [55].

We stress that the U -VCs is important only for low-frequencies $\omega \lesssim \min\{\omega_{\text{sf}}, \omega_{\text{cf}}\}$, where $\omega_{\text{sf(cf)}}$ is the characteristic spin (orbital/charge) fluctuation energy. Note that $\omega_{\text{sf(cf)}}$ becomes smaller near the quantum-critical-point in proportion to $1 - \alpha_{S(C)}$. Since the Cooper pair is formed by low-energy electrons, the U -VCs in $\hat{V}^\Lambda(k, p)$ play significant role on the superconducting state. On the other hand, the contribution of the U -VCs for the two susceptibilities in V^{cross} is expected to be small because of the frequency summation inside of V^{cross} : We verified this fact numerically in the present model.

Appendix B: Susceptibilities in the SC-VC theory

In the main text, we studied the FeSe model by applying the SC-VC theory introduced in Refs. [14, 22]. We analyzed the MT-VC and AL-VC for both spin- and charge-channels self-consistently. In the present theory, the charge (spin) susceptibilities are given as

$$\hat{\chi}^{c(s)}(\mathbf{q}) = \hat{\Phi}^{c(s)}(\mathbf{q})(\hat{1} - \hat{\Gamma}^{c(s)}\hat{\Phi}^{c(s)}(\mathbf{q}))^{-1} \quad (\text{B1})$$

where $\hat{\Phi}^{c(s)}(\mathbf{q})$ is given in Eq. (1) in the main text. It is rewritten as $\hat{\Phi}^x(\mathbf{q}) = \hat{\chi}^0(\mathbf{q}) + \hat{X}^{\text{MT},x}(\mathbf{q}) + \hat{X}^{\text{AL},x}(\mathbf{q})$, where $X^{\text{MT(AL)},x}$ represents the MT-VC (AL-VC).

The charge- and spin-channel AL-VCs are given as

$$\begin{aligned} X_{l,l';m,m'}^{\text{AL},c}(q) &= \frac{T}{2} \sum_p \sum_{a \sim h} \Lambda_{l,l';a,b;e,f}^0(q, p) \\ &\times \{3I_{a,b;c,d}^s(p+q)I_{e,f;g,h}^s(-p) + I_{a,b;c,d}^c(p+q)I_{e,f;g,h}^c(-p)\} \\ &\times \Lambda_{m,m';c,d;g,h}^{0'}(q, p), \end{aligned} \quad (\text{B2})$$

$$\begin{aligned} X_{l,l';m,m'}^{\text{AL},s}(q) &= \frac{T}{2} \sum_p \sum_{a \sim h} \Lambda_{l,l';a,b;e,f}^0(q, p) \\ &\times \{I_{a,b;c,d}^c(p+q)I_{e,f;g,h}^s(-p) \\ &+ I_{a,b;c,d}^s(p+q)I_{e,f;g,h}^c(-p)\} \Lambda_{m,m';c,d;g,h}^{0'}(q, p) \\ &+ \delta X_{l,l';m,m'}^{\text{AL},s}(q), \end{aligned} \quad (\text{B3})$$

where $\hat{I}^x(q) = \hat{U}^{0x}\hat{\chi}^x(q)\hat{U}^{0x} + \hat{U}^{0x}$, and $a \sim f$ are orbital indices. The three-point vertex $\Lambda_{l,l';a,b;e,f}^0(q, p)$ is given as $-T \sum_{k'} G_{l,a}(k'+q)G_{f,l'}(k')G_{b,e}(k'-p)$. Also, $\Lambda_{m,m';c,d;g,h}^{0'}(q, p) \equiv \Lambda_{c,h;m,g;d,m'}^0(q, p) + \Lambda_{g,d;m,c;h,m'}^0(q, -p-q)$. The last term in Eq. (B3) is

given as

$$\delta X_{l,l';m,m'}^{\text{AL},s}(q) = T \sum_p \sum_{a \sim h} \Lambda_{l,l';a,b,e,f}^0(q,p) \\ \times I_{a,b;c,d}^s(p+q) I_{e,f;g,h}^s(-p) \Lambda_{m,m';c,d;g,h}^{0''}(q,p) \quad (\text{B4})$$

where $\Lambda_{m,m';c,d;g,h}^{0''}(q,p) \equiv \Lambda_{c,h;m,g;d,m'}^0(q,p) - \Lambda_{g,d;m,c;h,m'}^0(q,-p-q)$. This term is found to be very small.

The expressions of the charge- and spin-channel MT-VCs are given in Ref. [65]. The double-counting second-order terms with respect to H_U in $\hat{X}^{\text{MT},s(c)} + \hat{X}^{\text{AL},s(c)}$ should be subtracted to obtain reliable results [65].

Figure 9 shows the relation between the spin and charge Stoner factors, α_S and α_C , in the 15% e -doped FeSe model obtained by the SC-VC theory for $r = 0 \sim 0.35$. Both spin- and charge-channel VCs are calculated self-consistently. Both α_S and α_C increase with r monotonically, and α_C exceeds α_S for $\alpha_{S,C} = 0.86$, since χ^s -square term in the charge-channel AL-VC in Eq. (B2) becomes significant for $\alpha_S \rightarrow 1$. For comparison, we show the Stoner factors in the case that the spin-channel VC is dropped and only the charge-channel VC are studied self-consistently, shown as the “charge-channel SC-VC” method. The obtained result is essentially similar to the “full SC-VC” method performed in the main text.

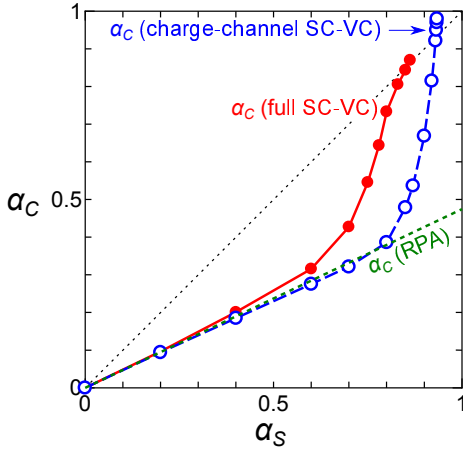


FIG. 9: (color online) Stoner factors obtained by the “full SC-VC” method performed in the main text. For comparison, the result given by the “charge-channel SC-VC” and that by the RPA are also shown.

Appendix C: Analysis of the original bulk FeSe tight-binding model

In the main text, we analyzed the heavily e -doped FeSe model introduced in the Method section. To reproduce the experimental bandstructure for high- T_c FeSe with heavily e -doping, we introduced the additional term ΔH_0 into the tight-binding model for bulk FeSe, as in Eq. (6). Here, we perform the same analysis for the original bulk

FeSe tight-binding model ($\Delta H_0 = 0$) with 15% e -doping, and obtain the s_{++} -wave state that is similar to Fig. 5 in the main text.

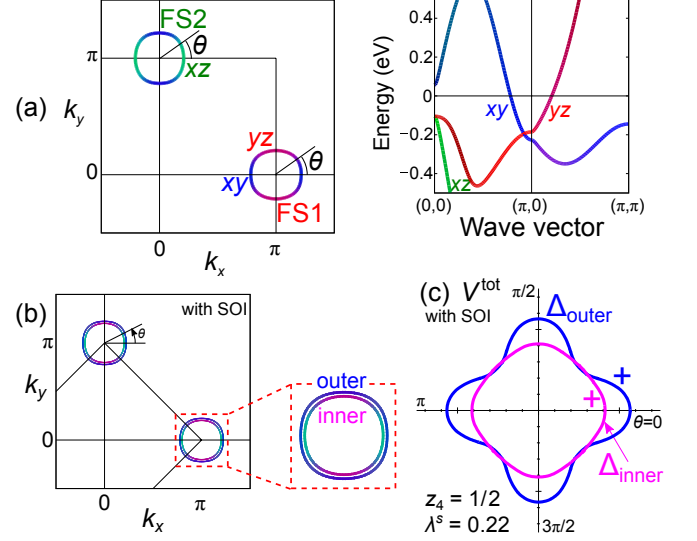


FIG. 10: (color online) (a) FSs and bandstructure of the bulk FeSe model ($\hat{H}_k^{0,b}$) with 15% e -doping. Green, red, and blue lines correspond to xz , yz , and xy orbitals, respectively. (b) FSs in the 2Fe-UC FeSe model for $\lambda_{\text{SOI}} = 80$ meV. The outer (inner) FS is mainly composed of the xy -orbital (xz , yz -orbitals). (c) The obtained s_{++} -wave gap function for V^{tot} in the case of $r = 0.36$ and $z_4 = 1/2$; $(\alpha_S, \alpha_C) = (0.83, 0.85)$.

Figure 10 (a) shows the FSs and bandstructure for the bulk FeSe model ($\Delta H_0 = 0$) with 15% e -doping. Here, the relation $E_{xy} < E_{yz}$ holds at X-point. The shape of the FSs is similar to that for the heavily e -doped FeSe model in the main text, shown in Fig. 2 (a). On the other hand, the Fermi velocity in Fig. 10 (a) is larger compared to Fig. 2 (a) in the main text. For this reason, the density-of-states at the Fermi level is relatively small in the present bulk FeSe tight-binding model. By applying the SC-VC method, we obtain the moderate incommensurate spin fluctuations and ferro-orbital fluctuations, which are essentially similar to those in the main text shown in Fig. 2(c). Figure 10 (b) shows the FSs in the 2Fe-UC model for $\lambda_{\text{SOI}} = 80$ meV. The outer (inner) FS is mainly composed of the xy -orbital (xz , yz -orbitals). Next, we study the superconducting state for the total pairing interaction V^{tot} given by the SC-VC theory. The obtained full-gap s_{++} -wave state is shown in Fig. 10 (c). Here, we put $r = 0.36$ and $z_4 = 1/2$ at $T = 30$ meV, in which the Stoner factors are $(\alpha_S, \alpha_C) = (0.83, 0.85)$.

Therefore, the full-gap s_{++} -wave state similar to Fig. 6 (f) in the main text is obtained by analyzing the bulk FeSe model $\hat{H}_k^{0,b}$ with 15% e -doping. On the other hand, the obtained eigenvalue is just $\lambda^s = 0.22$. This result indicates that the change in the bandstructure in monolayer FeSe, which is reproduced by ΔH_0 in the present Hamiltonian, is important to realize high- T_c superconductivity.

-
- [1] K. Kuroki, S. Onari, R. Arita, H. Usui, Y. Tanaka, H. Kontani, and H. Aoki, *Phys. Rev. Lett.* **101**, 087004 (2008).
- [2] I. I. Mazin, D. J. Singh, M. D. Johannes, and M. H. Du, *Phys. Rev. Lett.* **101**, 057003 (2008).
- [3] S. Graser, G. R. Boyd, C. Cao, H.-P. Cheng, P. J. Hirschfeld, and D. J. Scalapino, *Phys. Rev. B* **77**, 180514(R) (2008).
- [4] A. V. Chubukov, D. V. Efremov, and I. Eremin, *Phys. Rev. B* **78**, 134512 (2008).
- [5] H. Kontani and S. Onari, *Phys. Rev. Lett.* **104**, 157001 (2010).
- [6] Z. P. Yin, K. Haule, and G. Kotliar, *Nat. Phys.* **10**, 845 (2014).
- [7] H. Hosono and K. Kuroki, *Physica C* **514**, 399 (2015).
- [8] M. Yi, D. Lu, J.-H. Chu, J. G. Analytis, A. P. Sorini, A. F. Kemper, B. Moritz, S.-K. Mo, R. G. Moore, M. Hashimoto, W.-S. Lee, Z. Hussain, T. P. Devereaux, I. R. Fisher, and Z.-X. Shen, *Proc. Natl. Acad. Sci. USA* **108**, 6878 (2011).
- [9] Y. Zhang, C. He, Z. R. Ye, J. Jiang, F. Chen, M. Xu, Q. Q. Ge, B. P. Xie, J. Wei, M. Aeschlimann, X. Y. Cui, M. Shi, J. P. Hu, and D. L. Feng, *Phys. Rev. B* **85**, 085121 (2012).
- [10] C. Fang, H. Yao, W.-F. Tsai, J. P. Hu, and S. A. Kivelson, *Phys. Rev. B* **77**, 224509 (2008).
- [11] R. M. Fernandes, A. V. Chubukov, J. Knolle, I. Eremin, and J. Schmalian, *Phys. Rev. B* **85**, 024534 (2012).
- [12] F. Krüger, S. Kumar, J. Zaanen, and J. van den Brink, *Phys. Rev. B* **79**, 054504 (2009).
- [13] C.-C. Lee, W.-G. Yin, and W. Ku, *Phys. Rev. Lett.* **103**, 267001 (2009).
- [14] S. Onari and H. Kontani, *Phys. Rev. Lett.* **109**, 137001 (2012).
- [15] H. Kontani and Y. Yamakawa, *Phys. Rev. Lett.* **113**, 047001 (2014).
- [16] J. R. Schrieffer, *J. Low. Temp. Phys.* **99**, 397 (1995).
- [17] M. H. Sharifzadeh Amin and P. C. E. Stamp, *Phys. Rev. Lett.* **77**, 3017 (1996).
- [18] E. Bascones, B. Valenzuela, and M. J. Calderón, *Phys. Rev. B* **86**, 174508 (2012).
- [19] R. Yu and Q. Si, *Phys. Rev. Lett.* **110**, 146402 (2013).
- [20] N. Lanatà, H. U. R. Strand, G. Giovannetti, B. Hellsing, L. de' Medici, and M. Capone, *Phys. Rev. B* **87**, 045122 (2013).
- [21] L. de' Medici, G. Giovannetti, and M. Capone, *Phys. Rev. Lett.* **112**, 177001 (2014).
- [22] Y. Yamakawa, S. Onari, and H. Kontani, *Phys. Rev. X* **6**, 021032 (2016).
- [23] S. Onari, Y. Yamakawa, and H. Kontani, *Phys. Rev. Lett.* **116**, 227001 (2016).
- [24] Y. Yamakawa and H. Kontani, *Phys. Rev. Lett.* **114**, 257001 (2015).
- [25] M. Tsuchiizu, Y. Yamakawa, and H. Kontani, *Phys. Rev. B* **93**, 155148 (2016).
- [26] S. Sachdev and R. La Placa, *Phys. Rev. Lett.* **111**, 027202 (2013).
- [27] Y. Wang and A. Chubukov, *Phys. Rev. B* **90**, 035149 (2014).
- [28] J. K. Glasbrenner, I. I. Mazin, H. O. Jeschke, P. J. Hirschfeld, R. M. Fernandes, and R. Valentí, *Nat. Phys.* **11**, 953 (2015).
- [29] F. Wang, S. A. Kivelson, and D.-H. Lee, *Nat. Phys.* **11**, 959 (2015).
- [30] R. Yu and Q. Si, *Phys. Rev. Lett.* **115**, 116401 (2015).
- [31] A. V. Chubukov, M. Khodas, and R. M. Fernandes, *Phys. Rev. X* **6**, 041045 (2016).
- [32] K. Jiang, J. Hu, H. Ding, and Z. Wang, *Phys. Rev. B* **93**, 115138 (2016).
- [33] L. Fanfarillo, G. Giovannetti, M. Capone, and E. Bascones, *Phys. Rev. B* **95**, 144511 (2017).
- [34] S.-H. Baek, D. V. Efremov, J. M. Ok, J. S. Kim, J. van den Brink, and B. Büchner, *Nat. Mater.* **14**, 210 (2015).
- [35] A. E. Böhmer, T. Arai, F. Hardy, T. Hattori, T. Iye, T. Wolf, H. v. Löhneysen, K. Ishida, and C. Meingast, *Phys. Rev. Lett.* **114**, 027001 (2015).
- [36] S. Hosoi, K. Matsuura, K. Ishida, Hao Wang, Y. Mizukami, T. Watashige, S. Kasahara, Y. Matsuda, and T. Shibauchi, *Proc. Natl. Acad. Sci. USA* **113**, 8139 (2016).
- [37] P. Massat, D. Farina, I. Paul, S. Karlsson, P. Strobel, P. Toulemonde, M.-A. Méasson, M. Cazayous, A. Sacuto, S. Kasahara, T. Shibauchi, Y. Matsuda, and Y. Gallais, *Proc. Natl. Acad. Sci. USA* **113**, 9177 (2016).
- [38] Y. Suzuki, T. Shimojima, T. Sonobe, A. Nakamura, M. Sakano, H. Tsuji, J. Omachi, K. Yoshioka, M. Kuwata-Gonokami, T. Watashige, R. Kobayashi, S. Kasahara, T. Shibauchi, Y. Matsuda, Y. Yamakawa, H. Kontani, and K. Ishizaka, *Phys. Rev. B* **92**, 205117 (2015).
- [39] Q.-Y. Wang, Z. Li, W.-H. Zhang, Z.-C. Zhang, J.-S. Zhang, W. Li, H. Ding, Y.-B. Ou, P. Deng, K. Chang, J. Wen, C.-L. Song, K. He, J.-F. Jia, S.-H. Ji, Y.-Y. Wang, L.-L. Wang, X. Chen, X.-C. Ma, and Q.-K. Xue, *Chin. Phys. Lett.* **29**, 037402 (2012).
- [40] Y. Sun, W. Zhang, Y. Xing, F. Li, Y. Zhao, Z. Xia, L. Wang, X. Ma, Q.-K. Xue, and J. Wang, *Sci. Rep.* **4**, 6040 (2014).
- [41] J.-F. Ge, Z.-L. Liu, C. Liu, C.-L. Gao, D. Qian, Q.-K. Xue, Y. Liu, and J.-F. Jia, *Nat. Mater.* **14**, 285 (2015).
- [42] Q. Fan, W. H. Zhang, X. Liu, Y. J. Yan, M. Q. Ren, R. Peng, H. C. Xu, B. P. Xie, J. P. Hu, T. Zhang, and D. L. Feng, *Nat. Phys.* **11**, 946 (2015).
- [43] Y. Zhang, J. J. Lee, R. G. Moore, W. Li, M. Yi, M. Hashimoto, D. H. Lu, T. P. Devereaux, D.-H. Lee, and Z.-X. Shen, *Phys. Rev. Lett.* **117**, 117001 (2016).
- [44] Y. Miyata, K. Nakayama, K. Sugawara, T. Sato, and T. Takahashi, *Nat. Mater.* **14**, 775 (2015).
- [45] C. H. P. Wen, H. C. Xu, C. Chen, Z. C. Huang, Y. J. Pu, Q. Song, B. P. Xie, Mahmoud Abdel-Hafiez, D. A. Chareev, A. N. Vasiliev, R. Peng, and D. L. Feng, *Nat. Commun.* **7**, 10840 (2016).
- [46] Y. J. Yan, W. H. Zhang, M. Q. Ren, X. Liu, X. F. Lu, N. Z. Wang, X. H. Niu, Q. Fan, J. Miao, R. Tao, B. P. Xie, X. H. Chen, T. Zhang, and D. L. Feng, *Phys. Rev. B* **94**, 134502 (2016).
- [47] Z. Du, X. Yang, H. Lin, D. Fang, G. Du, J. Xing, H. Yang, X. Zhu, and H.-H. Wen, *Nat. Commun.* **7**, 10565 (2016).
- [48] D.-H. Lee, *Chin. Phys. B* **24**, 117405 (2015).
- [49] S. Rebec, T. Jia, C. Zhang, M. Hashimoto, D. Lu, R. Moore, and Z. Shen, *arXiv:1606.09358*.
- [50] S. Choi, W.-J. Jang, H.-J. Lee, J. M. Ok, H. W. Choi, A.

- T. Lee, A. Akbari, H. Suh, Y. K. Semertzidis, Y. Bang, J. S. Kim, and J. Lee, arXiv:1608.00886.
- [51] Y. Zhou and A. J. Millis, Phys. Rev. B **93**, 224506 (2016).
 - [52] L. Rademaker, Y. Wang, T. Berlijn, and S. Johnston, New J. Phys. **18**, 022001 (2016).
 - [53] T. Saito, S. Onari, and H. Kontani, Phys. Rev. B **83**, 140512 (2011).
 - [54] J. Kang and R. M. Fernandes, Phys. Rev. Lett. **117**, 217003 (2016).
 - [55] R. Tazai, Y. Yamakawa, M. Tsuchiizu, and H. Kontani, Phys. Rev. B **94**, 115155 (2016).
 - [56] T. Miyake, K. Nakamura, R. Arita, and M. Imada, J. Phys. Soc. Jpn. **79**, 044705 (2010).
 - [57] J. J. Seo, B. Y. Kim, B. S. Kim, J. K. Jeong, J. M. Ok, J. S. Kim, J. D. Denlinger, S.-K. Mo, C. Kim, and Y. K. Kim, Nat. Commun. **7**, 11116 (2016).
 - [58] Z. P. Yin, K. Haule, and G. Kotliar, Nat. Mater. **10**, 932 (2011).
 - [59] M. Khodas and A. V. Chubukov, Phys. Rev. Lett. **108**, 247003 (2012).
 - [60] T. Saito, Y. Yamakawa, S. Onari, and H. Kontani, Phys. Rev. B **92**, 134522 (2015).
 - [61] M. M. Hrovat, P. Jeglič, M. Klanjšek, T. Hatakeda, T. Noji, Y. Tanabe, T. Urata, K. K. Huynh, Y. Koike, K. Tanigaki, and D. Arčon, Phys. Rev. B **92**, 094513 (2015).
 - [62] N. Kawaguchi, N. Fujiwara, S. Iimura, S. Matsuishi, and H. Hosono, Phys. Rev. B **94**, 161104(R) (2016).
 - [63] S. Onari, Y. Yamakawa, and H. Kontani, Phys. Rev. Lett. **112**, 187001 (2014).
 - [64] Y. Yamakawa and H. Kontani, arXiv:1609.09618.
 - [65] S. Onari and H. Kontani, *Iron-Based Superconductivity*, (ed. P. D. Johnson, G. Xu, and W.-G. Yin, Springer-Verlag Berlin and Heidelberg GmbH & Co. K (2015)).